



Methylene blue degradation using chitosan-Fe₂O₃ composite and photo-Fenton

Abstract

This study aims to study the photodegradation process of methylene blue using a synthetic chitosan-Fe₂O₃ composite and their characterization. Based on the characterization material synthetic, chitosan-Fe₂O₃ (1:1) composite showed the best material with the smallest crystal size (1.13 nm), the surface morphology was lumpy and had an uneven shape with the composition of the constituent (Carbon (C) 42.88%, Oxygen (O) 48.68%, and Iron (Fe) 29.90%), and showed the smallest energy band gap (1.41 eV) which led us to conclude that the formation of the chitosan-Fe₂O₃ composite can reduce the energy band gap of Fe₂O₃. The best composite material then was used to evaluate the activity in degrading methylene blue. The optimum condition in degrading was reached at a contact time of 180 min and pH 9 with a percentage decrease in methylene blue concentration of 90.00%. The effect of concentration variations occurred at 5 ppm with a decrease of 89.62%. Total organic carbon analysis showed that the decrease in methylene blue concentration reached 92.20%. Based on that, it is concluded that the chitosan-Fe₂O₃ composite could be a potential alternative material to degrade methylene blue.

Keywords: chitosan-Fe₂O₃; methylene blue; chitosan; total organic carbon; photodegradation.

Degradación de azul de metileno usando material compuesto de quitosano-Fe₂O₃ y foto-Fenton

Resumen

Este estudio tiene como objetivo estudiar el proceso de fotodegradación del azul de metileno utilizando material sintético compuesto de quitosano-Fe₂O₃ y su caracterización. Con base en la caracterización del material sintético, el compuesto quitosano-Fe₂O₃ (1:1) mostró el mejor material con el tamaño de cristal más pequeño (1,13 nm), la morfología de la superficie era grumosa y tenía una forma desigual con la composición del constituyente (carbono (C) 42,88%, oxígeno (O) 48,68% y hierro (Fe) 29,90%), y mostró la banda prohibida de energía más pequeña (1,41 eV), lo que indica que la formación del compuesto de quitosano-Fe₂O₃ puede reducir la banda prohibida de energía de Fe₂O₃. Luego se utilizó el mejor material compuesto para ver su actividad en la degradación del azul de metileno. La condición óptima en la degradación se alcanzó con un tiempo de contacto de 180 min y pH 9 con una disminución porcentual en la concentración de azul de metileno del 90,00%. El efecto de las variaciones de concentración se presentó a 5 ppm con una disminución del 89,62%. El análisis de carbono orgánico total mostró que la disminución en la concentración de azul de metileno alcanzó el 92,20%. Con base en esto, se concluyó que el compuesto quitosano-Fe₂O₃ podría ser un material alternativo potencial para degradar el azul de metileno.

Palabras clave: quitosano-Fe₂O₃; azul de metileno; quitosano; carbono orgánico total; fotodegradación.

Degradação de azul de metileno usando composto de quitosana-Fe₂O₃ e foto-Fenton

Resumo

Este trabalho tem como objetivo estudar o processo de fotodegradação do azul de metileno utilizando material sintético composto quitosana-Fe₂O₃ e sua caracterização. Com base na caracterização do material sintético, o composto quitosana-Fe₂O₃ (1:1) apresentou o melhor material com o menor tamanho de cristal (1,13 nm), a morfologia da superfície era granulosa e apresentava formato irregular com a composição do constituinte (Carbono (C) 42,88%, Oxigênio (O) 48,68% e Ferro (Fe) 29,90%), e apresentou o menor gap de energia (1,41 eV) o que conclui que a formação do composto quitosana-Fe₂O₃ pode reduzir o band gap de energia de Fe₂O₃. O melhor material composto usado para ver sua atividade na degradação do azul de metileno. A condição ótima de degradação foi alcançada com tempo de contato de 180 minutos e pH 9 com diminuição percentual na concentração de azul de metileno de 90,00%. O efeito das variações de concentração ocorreu a 5 ppm com diminuição de 89,62%. A análise do carbono orgânico total mostrou que a diminuição da concentração de azul de metileno atingiu 92,20%. com base nisso, concluiu que o composto quitosana-Fe₂O₃ poderia ser um potencial material alternativo para degradar o azul de metileno.

Palavras-chave: quitosana-Fe₂O₃; azul de metileno; quitosana; carbono orgânico total; fotodegradação.

Introduction

Dyes are one of the important components in various industries such as paper, textiles, and cosmetics. Massive production from the rapid textile industry will certainly increase the magnitude of dye liquid waste. Therefore, they are feared to be one of the main contributors to water pollution [1]. The textile industry produces the largest amount of synthetic dye waste and produces around 50 to 200 mg/L dyes that could not be degraded entirely [2]. The type of dye that is widely used in the textile industry in Indonesia is methylene blue (MB) because it is a basic dye and has excellent solubility [3]. In the industry, only 5% of MB is bound, while the remaining 95% becomes waste; hence, its distribution in the aquatic environment is extensive [4]. Synthetic dyes are extremely hazardous to the environment and living creatures due to their poisonous, mutagenic, and carcinogenic qualities. The presence of a small number causes a decrease in water transparency and affects photosynthesis, as well as microbial activity of submerged organisms [5]. Cationic dyes are substantially more poisonous than their anionic counterpart because they can easily interact with negatively charged cell membranes, producing severe health issues [6]. MB, as one of the main cationic dyes, has been very worrying because, in high concentrations, it has a significant negative impact on various health problems [7].

Several methods, such as adsorption, biodegradation, and advanced oxidation process (AOP), have been studied extensively to reduce dye waste [8]. Among numerous treatment techniques of large-scale industrial wastewater containing persistent organics, the adsorption method is exceptional due to simple operations, low cost, and little secondary pollutions [9]. In recent years, several techniques are investigated to remove organic contaminants for wastewater remediation among which photocatalysis showed large opportunities due to the low energy consumption, complete decomposition of organic pollutants, and high stability [10, 11]. AOP methods, such as photo-Fenton, have attracted attention because they show excellent ability and activity in reducing dye concentration. Additionally, this method can degrade harmful compounds through an oxidation process with the help of Fenton reagent in the form of hydrogen peroxide and ultraviolet light [12]. The photo-Fenton process combines hydrogen peroxide and a catalyst to produce $\cdot\text{OH}$ radicals that decompose MB dye into molecules, such as CO₂, and water [13]. The transformation reaction takes place on the semiconductor material induced by ultraviolet light. The types often used for this process are iron semiconductors derived from the oxide, sulfide, carbide, and composite groups [14].

Fe₂O₃ is one of the semiconductors that have the potential to be used in dye degradation. A small bandgap makes this possible since the excitation energy required to move electrons from valence to conduction band is not excessive. However, the Fe₂O₃ semiconductor has a weakness in the separation process from the solution system because it is easily dispersed into water and tends to agglomerate and block the interaction with ultraviolet radiation [15]. One way to overcome this problem is by embedding Fe₂O₃ into a porous material such as chitosan. Chitosan is an adsorbent found in nature because it can be extracted from the shell waste of crustaceans such as shrimp and small crabs through the deacetylation process of chitin compounds [16]. As an adsorbent, chitosan has a functional group that acts as a ligand, making it more effective at the adsorption of polluting waste [17].

Research on composites doped with other compounds such as metals has developed a lot and has influenced the progress of research in the environmental field. Composite doped has been reported is chitosan-Al₂O₃ for thorium (IV), Pb (II) and Cd (II) adsorption [18, 19]. Heterogeneous photocatalysis is based on the absorption of radiant energy by semiconductor materials, causing redox reactions

and promoting organic degradation of pollutants. The most commonly used photocatalyst is a metal oxide as in this study was used Fe₃O₄ [20]. Based on research data that when a material is added Fe metal oxide compounds have an efficiency of almost 80%, provides a basis for the use of Fe₃O₄ material to be used as a photocatalyst [21, 22]. Other composite, chitosan-Fe₃O₄, resulted in a metronidazole removal efficiency of up to 100% [14]. Based on literature studies, there are no reports on the photodegradation of MB using chitosan-Fe₂O₃. In this study, chitosan-Fe₂O₃ composite with various mass ratios of (1:1), (1:2), and (1:3) was synthesized using the sol-gel method. The photo-Fenton system will then decompose MB using the composite under the optimal circumstances. Additionally, the effect of irradiation time and initial MB concentration was studied. The chitosan-Fe₂O₃ composite was characterized using X-ray diffraction (XRD), scanning electron microscopy-energy dispersive X-ray (SEM-EDX), and ultra violet-diffuse reflectance spectroscopy (UV-DRS), and the product of photodegradation was tested quantitatively using total organic carbon (TOC).

Materials and Methods

Materials

The materials used in the synthesis of chitosan-Fe₂O₃ composite are FeCl₃ (Merck), demineralized water (pure H₂O), NH₄OH (Merck), chitosan powder (Sigma Aldrich), and NaOH (Merck). For the pH point zero charge and MB degradation procedures, NaNO₃ (Merck), NaOH (Merck), HCl 37% (Merck), and synthetic MB were used as materials.

Synthesis of Fe₂O₃

Fe₂O₃ was synthesized using the co-precipitation method. Initially, a solution of Fe³⁺ precursor was prepared by dissolving 1.46 g of FeCl₃ in 100 mL of pure water. Furthermore, it was added with 12% of NH₄OH and constantly stirred until a Fe₂O₃ precipitate was formed at pH 10. The precipitate formed was washed and filtered several times before heating in an oven at 100 °C for 2 h, followed by calcination at 300 °C for 4 h.

Synthesis of chitosan-Fe₂O₃ composite

Chitosan-Fe₂O₃ was synthesized using the sol-gel method [19]. Initially, 0.24 g of the chitosan powder was dissolved in 30 mL of 2% acetic acid and constantly stirred until a gel was formed. The mixture was added with 30 mL of 0.1 M FeCl₃ solution followed by 1 M NaOH until the pH reached 11.2 and stirred at a speed of 520 rpm at 90 °C for 4 h. After forming a reddish-brown product, it was then left for 24 h. The precipitate was decanted, centrifuged, and washed five times with pure water before drying in an oven for 2 h and 30 min at 110 °C. This was followed by calcination at 300 °C for 4 h. The same procedure was conducted on different mass ratios of chitosan and Fe₂O₃, namely (1:2) and (1:3) (w/w). The solids were then characterized using XRD (Shimadzu), SEM-EDX (PhenomProX Desktop), and UV-DRS (Analytic Jena). The best results of the synthesis were used for the photodegradation of MB.

Determination of pH point zero charge (pH_{pzc})

About 30 mL of 0.01 NaNO₃ solution was put into each container set at a pH range of 2 to 12 using HCl or NaOH. Furthermore, 0.03 g of the composite was added and stirred using a shaker at 32 °C for 2 h. The mixture was then left for two days, and the final pH was measured using a pH meter from each solution. The pH_{pzc} value was obtained from the intersection point between the initial and final curves.

MB degradation study

The MB degradation study was conducted in batches using a 10-watt UV lamp at pH_{pzc} conditions. Briefly, 30 mL of MB with concentrations of 1, 2, 3, 4, and 5 ppm were added with 1 mL of 30%

(v/v) H₂O₂. About 0.03 g of chitosan-Fe₂O₃ was then added and stirred using a magnetic stirrer at 450 rpm and a temperature of 90 °C into the UV reactor, with an irradiation time of 30, 60, 120, and 180 min. The mixture was centrifuged for 10 min, and the absorbance of the filtrate was measured using a UV-Vis spectrophotometer (Orion™ AquaMate 8000) at a wavelength of 665 nm and analyzed using TOC (Torch Combustion Analyzer, Teledyne tekmar). The percentage (%) of MB degradation can be calculated using the following equation:

$$\text{Degradation MB (\%)} = \frac{X_0 - X_t}{X_0} \times 100\% \quad (1)$$

where X₀ is the initial concentration dye before irradiation and X_t is the concentration dye after irradiation. TOC calculation based on Eq. (1) is as follows:

$$\text{TOC Degradation (\%)} = \frac{C_0 - C_t}{C_0} \times 100\% \quad (2)$$

where C₀ is the initial concentration carbon (before degradation process) and C_t is the final concentration carbon (after degradation process).

Results and Discussion

Material chitosan-Fe₂O₃ composite characterization

Chitosan-Fe₂O₃ composite with various mass ratios of (1:1), (1:2), and (1:3) was characterized using XRD, SEM-EDX, and UV-DRS. The best result was applied to the photodegradation of MB. The photocatalyst diffractogram of chitosan, Fe₂O₃, and chitosan-Fe₂O₃ composite is shown in **figure 1**. **Figure 1A** shows that the typical diffraction peak of chitosan appears at an angle 2θ of 19.95°. Foroughnia *et al.* stated that the typical diffraction peak ranges from 10 to 20° [16], which is consistent with other findings [18]. Furthermore, **figure 1B** shows the diffraction peak at an angle 2θ of 24.13, 33.15, 54.09, 57.59, 62.41, 63.99 and 72.26° with field indexes of (012), (104), (110), (113), (024), (116), (018), (214), (300) and (119), indicating the presence of Fe₂O₃ compound (JCPDS card No. 33-0664). The diffraction peaks are consistent with previous reports [23].

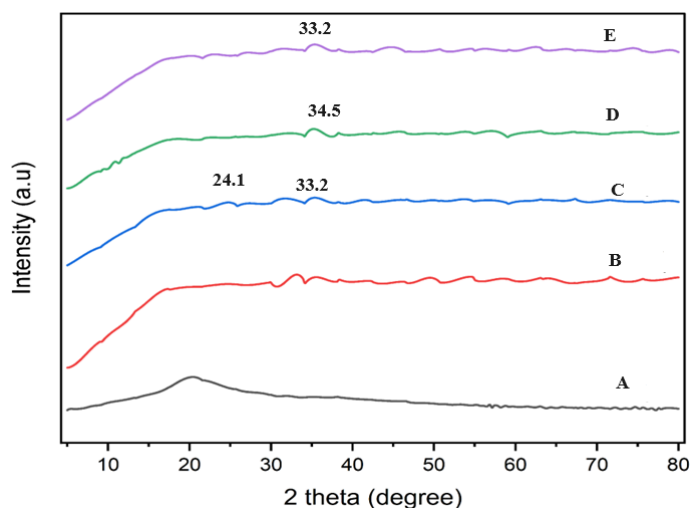


Figure 1. Diffractograms of A: Chitosan, B: Fe₂O₃, C: Chitosan-Fe₂O₃ Ratio 1:1, D: Chitosan Fe₂O₃ Ratio 1:2, and E: Chitosan-Fe₂O₃ Ratio 1:3.

Figure 1C shows that the diffraction peaks of the chitosan-Fe₂O₃ (1:1) composite appear at an angle 2θ of 24.1, 33.2, 62.2, and 74°. The diffractogram of the chitosan-Fe₂O₃ (1:2) composite in **figure 1D** shows the presence of a peak angle 2θ at 34.5, 57.4, 64.9 and 75.1°. Furthermore, the peaks at an angle 2θ of 16.9, 32.2, 54.5, and 74.7° appear on the diffractogram of the chitosan-Fe₂O₃ (1:2) composite, as shown in **figure 1E**. Chitosan-Fe₂O₃ (1:1), (1:2), and (1:3) composite did not specifically indicate the presence of chitosan peaks. This is probably due to a decrease in intermolecular hydrogen bonds since Fe₂O₃ dominates. This condition indicates a good interaction between Fe₂O₃ and the structure of chitosan [24].

The angle 2θ and the intensity peak of each composite are shown in table 1. The composite with a mass ratio of (1:1) showed the highest intensity. Based on the Debye-Scherrer equation, the crystal size of the chitosan-Fe₂O₃ composite with mass ratios of (1:1), (1:2), and (1:3) was 1.13, 2.82 and 8.83 nm, respectively. Therefore, the Fe₂O₃-composite (1:1) was selected for the MB photodegradation application. This is because of its smallest crystal size, high intensity, and the 2θ peak closest to JCPDS card No. 33-0664.

Table 1. 2θ value, peak intensity and crystallite size of chitosan-Fe₂O₃ composite.

Material	2θ (degree)	Peak intensity (cps)	Crystallite size (nm)
Chitosan-Fe ₂ O ₃ (1:1)	33.2	522	1.13
Chitosan-Fe ₂ O ₃ (1:2)	34.5	90	2.82
Chitosan-Fe ₂ O ₃ (1:3)	32.2	173	8.83

Characterization using UV-Vis DRS aims to determine the energy band gap of Fe₂O₃ and chitosan-Fe₂O₃ composite. The bandgap is defined as the distance from the valence to the conduction band of a semiconductor. **Table 2** shows the UV-Vis DRS analysis results. The energy band gaps of Fe₂O₃ and chitosan-Fe₂O₃ are 1.93 and 1.41 – 1.64 eV. Vayssieres *et al.* stated that the energy band gap of pure Fe₂O₃ ranges from 1.93 to 2.20 eV depending on the crystal state and the preparation method [25]. **Table 2** shows that the energy band gap of Fe₂O₃ decreases after forming the composite with chitosan. Similar findings have been reported by other studies [26]. According to Fauzi *et al.*, the decrease was associated with a smaller crystal size of the photocatalyst [27]. This leads to an increase in the orbital overlap between the valence and conduction bands. Furthermore, the energy band gap can inversely affect the photocatalytic effectiveness [28].

Table 2. Analysis bandgap energy of composites.

Material	Eg (eV)
Fe ₂ O ₃	1.93
Chitosan-Fe ₂ O ₃ (1:1)	1.41
Chitosan-Fe ₂ O ₃ (1:2)	1.50

The size of the band gap energy value in a composite greatly influences the degradation effect of a dye. The smaller the bandgap energy value, the better the dye degradation effect of the composite because it allows the formation of a large number of charge carriers under light irradiation [29]. A small band gap also provides less relaxation time for recombining electron and hole pairs, so that photodegradation carried out by composites with a small band gap is more favorable for degrading dyes [30]. Based on XRD and UV-DRS characterization, best composite we had is chitosan-Fe₂O₃ (1:1) and was carried out to SEM characterization to see the surface morphology of the composite. The surface morphology of chitosan and chitosan-Fe₂O₃ composite is shown in **figure 2**.

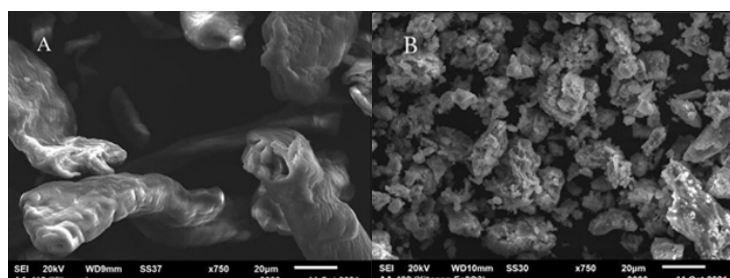


Figure 2. SEM Micrographs of A: Chitosan and B: Chitosan-Fe₂O₃.

It shows flakes or sheets that have pores with a magnification of 750×. The surface morphology of the chitosan-Fe₂O₃ composite shows the distribution and aggregation of Fe₂O₃ in chitosan. Many pores and folds are found in the composite, which can support photocatalytic activity. Similar morphology features were reported by Mendis *et al.* at synthetic material chitosan-ilmenite sand which

was used to photodegradation of MB dye with presenced aggregated spherical nanoparticles [31]. The EDX analysis results of chitosan and chitosan-Fe₂O₃ composite are shown in Table 3. It can be seen that the element Fe increases from 0 to 29.96% after forming a composite with chitosan. This indicates that Fe₂O₃ has successfully modified chitosan.

Table 3. Elemental analysis by EDX.

Element	Atomic (wt%)	
	Chitosan	Chitosan-Fe ₂ O ₃
C	42.88	27.19
O	48.68	25.27
Na	8.44	9.03
Cl	-	7.49
Fe	-	29.96
Zn	-	1.06

The pH_{pzc} is a surface state of neutral charge, pH_{pzc} greatly affects the adsorption of the dye with the catalyst surface on photodegradation [32]. The resulting pH_{pzc} data will be used in the MB photodegradation process. The pH_{pzc} of chitosan-Fe₂O₃ (1:1) composite can be seen in figure 3, which shows that the pH_{pzc} of the chitosan-Fe₂O₃ (1:1) composite is at pH 8. The catalyst's surface will be negative when $pH > pH_{pzc}$ hence it can degrade cationic dyes and vice versa [33]. In this study, MB dye is cationic, and its pH is set above pH_{pzc} before the photodegradation process is conducted. Since the composite surface is negative at high pH, it attracts the cationic dyestuff due to electrostatic interaction and the dye is adsorbed onto the composite surface.

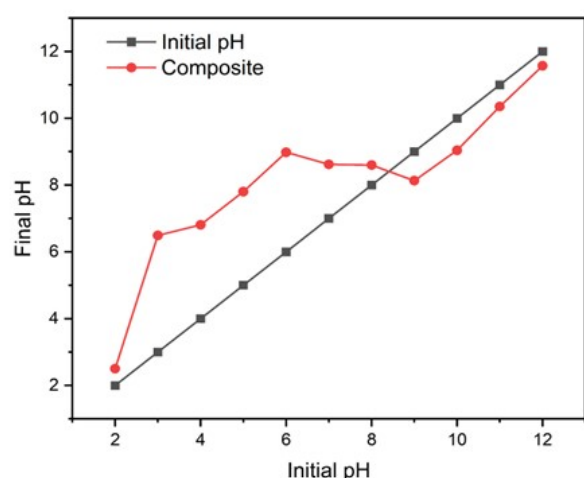


Figure 3. pH_{pzc} of chitosan-Fe₂O₃ (1:1).

MB photodegradation

MB degradation in this research was done using composite chitosan-Fe₂O₃ (1:1). This chitosan-Fe₂O₃ composite (1:1) was used because the characterization is the best result from the three composite generated materials. According to Zhang *et al.*, as the band gap energy is smaller in semiconductors, they can capture more photons for adsorption, so the theory will give the best result for chitosan-Fe₂O₃ composite on degradation of MB [34]. The effect of irradiation time on the decrease in MB concentration at a dye of 5 ppm is shown in figure 4. It shows that the highest and lowest percentage of decrease in MB concentration was achieved at an irradiation time of 180 and 30 min by 90.00 and 76.84% (gray line). Observations with a similar trend have been reported by Fassi *et al.* in a comparative study on the photodegradation of bromocresol green using Fe(II)/H₂O₂ and UV [35]. This condition shows that the degradation time is directly related to the contact between the photon rays and the chitosan-Fe₂O₃ composite, leading to a greater decrease in MB concentration. The presence of H₂O₂ acts as a reactant capable of producing hydroxyl radicals (•OH) which can degrade MB more effectively [12].

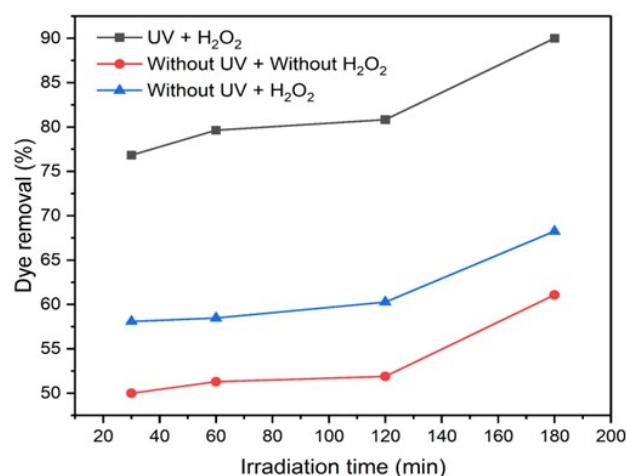
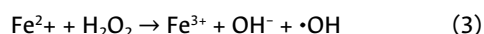


Figure 4. Effect irradiation time on methylene blue removal.

Control studies involving the degradation of MB without UV irradiation and without adding H₂O₂ (comparator I, red line) and without UV irradiation but adding H₂O₂ (comparator II, blue line) were carried out. Based on figure 4, the adsorption process without H₂O₂ (red line) showed the lowest percentage of decrease in MB concentration as compared to the UV irradiation process with H₂O₂ (blue line). The comparator I showed a degradation of 61.07%, while the comparator II was 68.26%. The difference between comparator II and photodegradation in the presence of H₂O₂ was 21.74%. This indicates that the addition of H₂O₂ greatly affects the MB degradation process.

The effect of the initial MB concentration on the decrease in MB concentration at an irradiation time of 180 min is shown in figure 5. It shows that the percentage decrease in MB concentration increased as the initial MB concentration increased. According to Shaban *et al.*, the addition of H₂O₂ is very influential in photodegradation because it is a reactant that produces •OH radicals for degrading dyes [36]. The •OH radicals produced are directly proportional to the amount of degraded MB dye. Furthermore, the combination of H₂O₂ with Fe³⁺, which acts as a homogeneous Fenton catalyst, can form •OH radicals. The Fenton oxidation reaction can be written based on Eq. (3) as follows:



The percentage of decrease in MB concentration was also achieved in comparator I through an adsorption process. The concentration of the dye determines the amount adsorbed on the surface of the composite [37]. A considerable increase in dye drop was also observed in the photodegradation trial without H₂O₂ (comparator II) at the initial MB concentration of 1 to 2 ppm. However, at the initial MB concentration of 3 ppm, the decrease of MB dye did not occur effectively. According to Jesse *et al.*, the higher the dye concentration, the more molecules are adsorbed on the catalyst's surface [38]. Consequently, they will inhibit the interaction between the catalyst and UV light. The formation of hydroxyl radicals on the catalyst's surface becomes constant and tends to act as an adsorbent at high concentrations.

Based on figure 5, the initial MB concentration of 5 ppm shows equilibrium with the adsorption and photodegradation processes without H₂O₂ of 55.28% and 69.60%, respectively. A significant difference in the percentage of decrease was observed with the addition of H₂O₂. The photodegradation process is higher than the adsorption because the UV light used has a role in producing •OH radicals, which can degrade MB. Without UV irradiation, the dye can only undergo the adsorption process [39]. Therefore, the effectiveness of photodegradation will increase with the addition of H₂O₂ to produce •OH radicals. In conclusion, the addition of H₂O₂ can affect

the effectiveness of photodegradation under the influence of the initial MB concentration. This is based on the photo-Fenton process, there are two reactions, namely Fenton and photocatalysis, where both reactions produce $\cdot\text{OH}$ radicals.

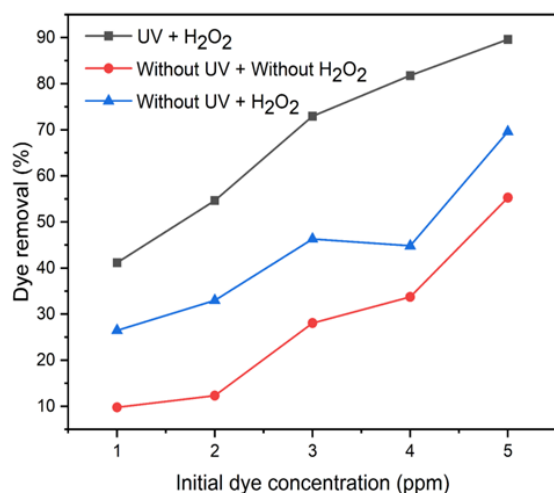


Figure 5. Effect of initial dye concentration on methylene blue removal.

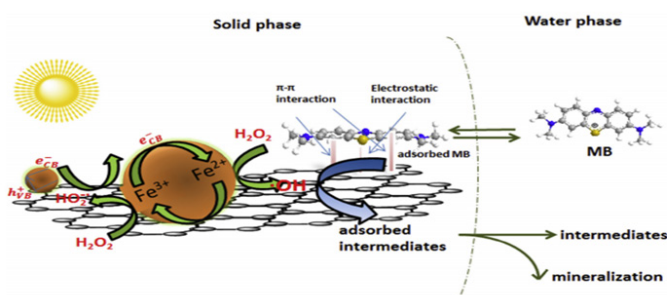


Figure 6. Schematic of photo-Fenton mechanism.

In figure 6 there are two reactions at once, the one where Fe^{2+} ions reacts with H_2O_2 using additional UV light to obtain Fe^{3+} ions and $\cdot\text{OH}$ radicals, and the other one where these $\cdot\text{OH}$ radicals will degrade MB dye. When there is electron excitation due to the photocatalyst reaction, there is a gap that can be entered by fenton radicals. The photocatalyst process also produces $\cdot\text{OH}$ radicals which results in an increase in the number of radicals obtained, so that degraded MB also increases along with increasing the number of radicals. After degradation of MB, the adsorption process occurs by chitosan as an adsorbent.

TOC analysis was conducted to determine the quantitative degradation of organic compounds based on absorbance. Figure 7 shows the test results before and after MB photodegradation. The decrease in absorbance was due to the decomposition process using chitosan- Fe_2O_3 (1:1) composite, directly related to C concentration in MB from 0.6493 to 0.0506 ppm (table 4). Based on these results, it shows that the composite could degrade MB and the percentage of degradation is 92.24%. Fe_2O_3 attach to chitosan improves the degradation activity of MB. Selpiana et al. in their research on the pho-

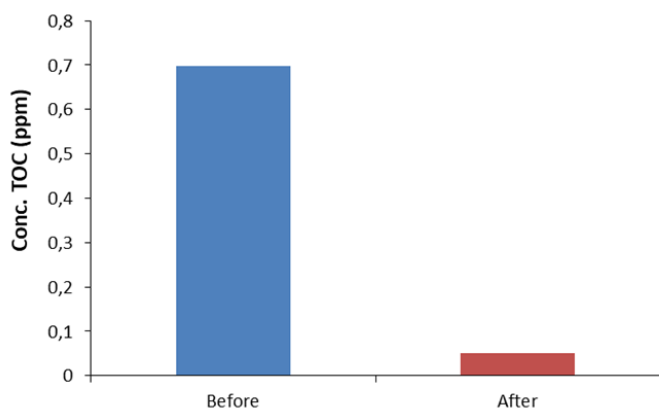


Figure 7. TOC Analysis of before and after degradation of MB with composite.

tocatalytic effect of MB degradation using Fe_2O_3 on heterojunction composite, state that Fe_2O_3 increases the capacity of the composite as a dye degrader by synergizing with other composites to reduce the energy band gap, so that photons will be captured more [40].

Table 4. TOC data and the concentration of total carbon.

Methylene blue	Adjust (Abs)	Concentration (ppm)
Before degradation	48.89	0.6493
After degradation	47.15	0.0506

Conclusions

Chitosan- Fe_2O_3 composite with mass ratios of (1:1), (1:2), and (1:3) has been successfully synthesized. XRD characterization showed that the chitosan- Fe_2O_3 (1:1) composite produced the smallest crystal size of 1.13 nm. Meanwhile, the UV-DRS analysis reported that Fe_2O_3 experienced an energy bandgap reduction after forming the chitosan- Fe_2O_3 composite. This was achieved in the chitosan- Fe_2O_3 (1:1) composite of 1.41 eV. SEM-EDX characterization showed the surface of chitosan in flakes with pores and chitosan- Fe_2O_3 , which tended to form lumps. The best condition for reducing MB concentration was achieved at an irradiation time of 180 min with an initial dye of 5 ppm and a percentage of decrease in MB at 90.00 and 89.62%. TOC analysis showed that the percentage of MB degradation obtained was 92.20%. Therefore, the chitosan- Fe_2O_3 composite has the potential as a photocatalyst to degrade MB.

Acknowledgment

The research publication of this article was funded by DIPPA of Public Service Agency of Universitas Sriwijaya 2022. SP DIPAO23.17.2.677515/2022, on December 13, 2021. In accordance with the Rector's Decree 0109/UN9.3.1/SK/2022, on April 28, 2022.

References

- [1] M. T. Yagub, T. K. Sen, S. Afroze and H. M. Ang, "Dye and its removal from aqueous solution by adsorption: a review", *Adv. Colloid Interface Sci.*, vol. 209, pp. 172–184, 2014. DOI: <https://doi.org/10.1016/j.cis.2014.04.002>
- [2] M. Mondal and S. De, "Treatment of textile plant effluent by hollow fiber nanofiltration membrane and multi-component steady state modeling", *Chemical Engineering Journal*, vol. 285, pp. 304–318, Feb. 2016. DOI: <https://doi.org/10.1016/j.cej.2015.10.005>.
- [3] L. Ai, Y. Zhou and J. Jiang, "Removal of methylene blue from aqueous solution by montmorillonite/CoFe₂O₄ composite with magnetic separation performance", *Desalination*, vol. 266, no. 1–3, pp. 72–77, Jan. 2011. DOI: <https://doi.org/10.1016/j.desal.2010.08.004>.
- [4] S. Chin, E. Park, M. Kim and J. Jurng, "Photocatalytic degradation of methylene blue with TiO₂ nanoparticles prepared by a thermal decomposition process", *Powder Technol.*, vol. 201, no. 2, pp. 171–176, Jul. 2010. DOI: <https://doi.org/10.1016/j.powtec.2010.03.034>.
- [5] H. Karaer and I. Kaya, "Synthesis and characterization of magnetic ZnCl₂-activated carbon produced from coconut shell for the adsorption of methylene blue", *Microporous Mesoporous Mater.*, vol. 232, pp. 26–38, 2021. DOI: <https://doi.org/10.1016/j.molstruc.2021.130071>
- [6] O. Duman, S. Tunç, T. G. Polat and B. K. I. Bozoğlan, "Synthesis of magnetic oxidized multiwalled carbon nanotube-κ-carrageenan-Fe₃O₄ nanocomposite adsorbent and its application in cationic Methylene Blue dye adsorption", *Carbohydr. Polym.*, vol. 147, pp. 79–88, 2016. DOI: <https://doi.org/10.1016/j.carbpol.2016.03.099>
- [7] H. Mittal, N. Ballav and S. B. Mishra, "Gum ghatti and Fe₃O₄ magnetic nanoparticles based nanocomposites for the effective adsorption of methylene blue from aqueous solution", *Ind. Eng. Chem. Res.*, vol. 20, no. 4, pp. 2184–2192, 2014. DOI: <https://doi.org/10.1016/j.icer.2014.03.002>

- doi.org/10.1016/j.jiec.2013.09.049
- [8] R. A. Solano, L. D. De León, G. De Ávila and A. P. Herrera, "Polycyclic aromatic hydrocarbons (PAHs) adsorption from aqueous solution using chitosan beads modified with thiourea, TiO₂ and Fe₃O₄ nanoparticles", *Environ. Technol. Innov.*, vol. 21, pp. 101378, 2021. DOI: <https://doi.org/10.1016/j.eti.2021.101378>
- [9] R. Wang et al., "Fabrication of a corn stalk derived cellulose-based bio-adsorbent to remove Congo red from wastewater: Investigation on its ultra-high adsorption performance and mechanism", *Int J Biol Macromol*, vol. 241, pp. 1–10, 2023. DOI: <https://doi.org/10.1016/j.ijbiomac.2023.124545>
- [10] Q. Wang, H. Li, X. Yu, Y. Jia, Y. Chang and S. Gao, "Morphology regulated Bi₂WO₆ nanoparticles on TiO₂ nanotubes by solvothermal Sb³⁺ doping as effective photocatalysts for wastewater treatment", *Electrochim Acta*, vol. 330, pp. 1–12, 2020. DOI: <https://doi.org/10.1016/j.electacta.2019.135167>
- [11] S. Sarkar, N. T. Ponce, A. Banerjee, R. Bandopadhyay, S. Rajendran and E. Lichtfouse, "Green polymeric nanomaterials for the photocatalytic degradation of dyes: a review", *Environmental Chemistry Letters*, vol. 18, pp. 1569–1580, 2020. DOI: <https://doi.org/10.1007/s10311-020-01021-w>
- [12] S. Shekar, G. C. K. Alkanad, A. Hezam, A. Alsalmeh, N. Al-Zaqri and N. K. Lokanath, "Enhanced photo-fenton activity over a sunlight-driven ignition synthesized A-Fe₂O₃-Fe₃O₄/CeO₂ heterojunction catalyst enriched with oxygen vacancies", *J. Mol. Liq.*, vol. 335, pp. 1–6, 2021. DOI: <https://doi.org/10.1016/j.molliq.2021.116186>
- [13] G. Zanchettin, G. S. Falk, S. Y. G. González and D. Hotza, "High performance magnetically recoverable Fe₃O₄ nanocatalysts: fast microwave synthesis and photo-fenton catalysis under visible-light", *Chem. Eng. Process. Intensif.*, vol. 166, pp. 1–8, 2021. DOI: <https://doi.org/10.1016/j.cep.2021.108438>
- [14] W. He, Z. Li, S. Lv, M. Niu, W. Zhou, J. Li, R. Lu, H. Gao, C. Pan and S. Zhang, "Facile synthesis of Fe₃O₄@MIL-100(Fe) towards enhancing photo-Fenton like degradation of levofloxacin via a synergistic effect between Fe₃O₄ and MIL-100(Fe)", *Chem. Eng. J.*, vol. 409, pp. 1–13, 2021. DOI: <https://doi.org/10.1016/j.cej.2020.128274>
- [15] A. Abharya and A. Gholizadeh, "Synthesis of a Fe₃O₄-rGO-ZnO-catalyzed photo-Fenton system with enhanced photocatalytic performance", *Ceram. Int.*, vol. 47, pp. 12010–12019, 2021. DOI: <https://doi.org/10.1016/j.ceramint.2021.01.044>
- [16] A. Foroughnia, A. D. Khalaji, E. Kolvari and N. Koukabi, "Synthesis of new chitosan Schiff base and its Fe₂O₃ nanocomposite: Evaluation of methyl orange removal and antibacterial activity", *Int. J. Biol. Macromol.*, vol. 177, pp. 83–91, 2021. DOI: <https://doi.org/10.1016/j.ijbiomac.2021.02.068>
- [17] L. M. Zhao, L. E. Shi, Z. L. Zhang, J. M. Chen, D. D. Shi, J. Yang and Z. X. Tang, "Preparation and application of chitosan nanoparticles and nanofibers", *Brazilian J. Chem. Eng.*, vol. 28, pp. 353–362, 2011. DOI: <https://doi.org/10.1590/S0104-66322011000300001>
- [18] B. R. Broujeni, A. Nilchi, A. H. Hassani and R. Saberi, "Application of chitosan/Al₂O₃ nano composite for the adsorption of thorium (IV) ion from aqueous solution", *Water Sci. Technol.*, vol. 78, pp. 708–720, 2018. DOI: <https://doi.org/10.5004/dwt.2018.21760>
- [19] R. Ahmad and A. Mirza, "Facile one pot green synthesis of chitosan-iron oxide (CS-Fe₂O₃) nanocomposite: removal of Pb(II) and Cd(II) from synthetic and industrial wastewater", *J. Clean. Prod.*, vol. 186, pp. 342–352, 2018. DOI: <https://doi.org/10.1016/j.jclepro.2018.03.075>
- [20] M. Coronell, G. Toscano-Lucas, R. Solano and A. Herrera, "Green Synthesis of Silver-Doped Titanium Dioxide Nanostructures for Acetaminophen Degradation Under Solar Radiation", *Ingeniería Y Universidad*, vol. 26, pp. 1–19, 2022. DOI: <https://doi.org/10.11144/Javeriana.iued26.gsst>
- [21] R. A. Solano, L. D. De León, G. De Ávila and A. P. Herrera, "Polycyclic aromatic hydrocarbons (PAHs) adsorption from aqueous solution using chitosan beads modified with thiourea, TiO₂ and Fe₃O₄ nanoparticles", *Environ Technol Innov.*, vol. 21, pp. 1–15, 2021. DOI: <https://doi.org/10.1016/j.eti.2021.101378>
- [22] R. A. Solano Pizarro and A. P. Herrera Barros, "Cypermethrin elimination using Fe-TiO₂ nanoparticles supported on coconut palm spathe in a solar flat plate photoreactor", *Advanced Composites Letters*, vol. 29, pp. 1–13, 2020. DOI: <https://doi.org/10.1177/2633366X20906164>
- [23] M. Alagiri and S. B. A. Hamid, "Sol-gel synthesis of α-Fe₂O₃ nanoparticles and its photocatalytic application", *Sol-Gel Sci. Technol.*, vol. 74, pp. 783–789, 2015. DOI: <https://doi.org/10.1007/s10971-015-3663-y>
- [24] M. B. Badry, M. A. Wahba, R. K. Khaled and M. Moawad, "Hydrothermally Assisted Synthesis of Magnetic Iron Oxide-Chitosan Nanocomposites: Electrical and Biological Evaluation", *Biointerface Res. Appl. Chem.*, vol. 12, pp. 2229–2241, 2022. DOI: <https://doi.org/10.33263/BRIAC122.22292241>
- [25] L. Vayssieres, C. Sathe, S. M. Butorin, D. K. Shuh, J. Nordgren and J. Guo, "One-Dimensional Quantum-Confinement Effect in α-Fe₂O₃ Ultrafine Nanorod Arrays", *Adv. Mater.*, vol. 17, pp. 2320–2323, 2005. DOI: <https://doi.org/10.1002/adma.200500992>
- [26] A. Badawi, E. M. Ahmed, N. Y. Mostafa, F. Abdel-Wahab and S. E. Alomairy, "Enhancement of the optical and mechanical properties of chitosan using Fe₂O₃ nanoparticles", *J. Mater. Sci. Mater. Electron.*, vol. 28, pp. 10877–10884, 2017. DOI: <https://doi.org/10.1007/s10854-017-6866-x>
- [27] N. I. M. Fauzi, Y. W. Fen, N. A. S. Omar, S. Saleviter, W. M. E. M. M. Daniyal, H. S. Hashim and M. Nasrullah, "Nanostructured chitosan/maghemite composites thin film for potential optical detection of mercury ion by surface plasmon resonance investigation", *Polymers*, vol. 12, pp. 1–13, 2020. DOI: <https://doi.org/10.3390/polym12071497>
- [28] F. Chai, K. Li, C. Song and X. Guo, "Synthesis of magnetic porous Fe₃O₄/C/Cu₂O composite as an excellent photo-Fenton catalyst under neutral condition", *J Colloid Interface Sci.*, vol. 475, pp. 119–125, 2016. DOI: <https://doi.org/10.1016/j.jcis.2016.04.047>
- [29] R. Khurram, Z. Wang, M. F. Ehsan, S. Peng, M. Shaffiq and B. Khan, "Synthesis and characterization of an α-Fe₂O₃/ZnTe heterostructure for photocatalytic degradation of Congo red, methyl orange and methylene blue", *RSC Adv.*, vol. 10, pp. 44997–45007, 2020. DOI: <https://doi.org/10.1039/D0RA06866G>
- [30] M. A. Bhatti, A. A. Shah, K. F. Almaani, A. Tahira, A. D. Chandio, M. Willander, O. Nur, A. Q. Mugheri, A. L. Bhatti, B. Waryani, A. Nafady and Z. H. Ibupoto, "TiO₂/ZnO Nanocomposite Material for Efficient Degradation of Methylene Blue", *Journal of Nanoscience and Nanotechnology*, vol. 21, pp. 2511–2519, 2021. DOI: <http://doi.org/10.1166/jnn.2021.19107>
- [31] A. Mendis, C. Thambiliyagodage, G. Ekanayake, H. Liyanaarachchi, M. Jayanetti and S. Vigneswaran, "Fabrication of Naturally Derived Chitosan and Ilmenite Sand-Based TiO₂/Fe₂O₃/Fe-N-Doped Graphitic Carbon Composite for Photocatalytic Degradation of Methylene Blue under Sunlight", *Molecules*, vol. 28, pp. 1–25, 2023. DOI: <http://doi.org/10.3390/molecules28073154>
- [32] Y. D. Shahamat, M. Sadeghi, A. Shahryari, N. Okhovat, F. B. Asl and M. M. Baneshi, "Heterogeneous catalytic ozonation of 2, 4-dinitrophenol in aqueous solution by magnetic carbonaceous nanocomposite: catalytic activity and mechanism", *Desalination and Water Treatment*, vol. 57, pp. 20447–20456, 2016. DOI: <http://doi.org/10.1080/19443994.2015>
- [33] H. Zhang, J. Liu, T. Xu, W. Ji and X. Zong, "Recent Advances on Small Band Gap Semiconductor Materials (≤2.1 eV) for Solar Water Splitting", *Catalysts*, vol. 13, pp. 728, 2023. DOI: <http://doi.org/10.3390/catal13040728>
- [34] Y. D. Shahamat, M. Sadeghi, A. Shahryari, N. Okhovat, F. Bahrami and M. M. Baneshi, "Heterogeneous catalytic ozonation

- of 2,4-dinitrophenol in aqueous solution by magnetic carbonaceous nanocomposite: Catalytic activity and mechanism Desalin", *Water Treat.*, vol. 57, pp. 20447–20456, 2016. DOI: <https://doi.org/10.1080/19443994.2015.1115372>
- [35] S. Fassi, K. Djebbar, I. A-Bousnoubra, H. Chenini and T. Sehili, "Oxidation of bromocresol green by different advanced oxidation processes: Fenton, Fenton-like, photo-Fenton, photo-Fenton-like and solar light. Comparative study", *Desalin. Water Treat.*, vol. 52, pp. 4982–4982, 2014. DOI: <https://doi.org/10.1080/19443994.2013.809971>
- [36] M. Shaban, M. R. Abukhadra, S. S. Ibrahim and M. G. Shahien, "Photocatalytic degradation and photo-Fenton oxidation of Congo red dye pollutants in water using natural chromite—response surface optimization", *Appl. Water Sci.*, vol. 7, pp. 4743–4756, 2017. DOI: <https://doi.org/10.1007/s13201-017-0637-y>
- [37] J. Shu, Z. Wang, Y. Huang, N. Huang, C. Ren and W. J. Zhang, "Adsorption Removal of Congo Red from aqueous solution by polyhedral Cu₂O nanoparticles: Kinetics, isotherms, thermodynamics and mechanism analysis", *Alloys Compd.*, vol. 633, pp. 338–346, 2015. DOI: <https://doi.org/10.1016/j.jallcom.2015.02.048>
- [38] K. A. Isai and V. S. Shrivastava, "Photocatalytic degradation of methylene blue using ZnO and 2%Fe–ZnO semiconductor nanomaterials synthesized by sol–gel method: a comparative study", *SN Appl. Sci.*, vol. 1, pp. 1–11, 2019. DOI: <https://doi.org/10.1007/s42452-019-1279-5>
- [39] A. Hou, B. Hu and J. Zhu, "Photocatalytic Degradation of Methylene Blue over TiO₂ Pretreated with Varying Concentrations of NaOH", *Catalysts*, vol. 8, pp. 1–13, 2018. DOI: <https://doi.org/10.3390/catal8120575>
- [40] H. Selpiana, A. B. Aritonang, M. A. Wibowo, W. Warsidah and A. Adhitiawarman, "Photocatalytic Degradation Of Methylene Blue Using Fe₂O₃-TiO₂/Kaolinite Under Visible Light Illumination", *JKPK*, vol. 7, pp. 277–286. DOI: <https://doi.org/10.20961/jkpk.v7i3.66567>

Article citation:

Desnelli, K. Ramadhina, D. Alfarado, Fatma, A. Mara and M. Said, "Methylene blue degradation using chitosan-Fe₂O₃ composite and photo-Fenton", *Rev. Colomb. Quim.*, vol. 52, no. 2, pp. 36–42, 2023. DOI: <https://doi.org/10.15446/rev.colomb.quim.v52n2.109625>